Harmonic Detection Method of Three-Phase Four-Wire APF Based on p-q-r Without Voltage-Sensor

Li Delu[1](✉), Liu Zhijian[1], Zhang Kailiang[2], and Hao Shaolong[1]

[1] Jiangsu Vocational Institute of Architectural Technology, Xuzhou, China
[2] Jiangsu Province Key Laboratory of Intelligent Industry Control Technology, Xuzhou University of Technology, Xuzhou, China

Abstract. The harmonic detection method based on $p-q-r$ defines the instantaneous power of zero-order current under the new spatial coordinate system, which can eliminate the midline current independently. This paper introduces the principle of the detection method and puts forward the $p-q-r$ method of harmonic detection without voltage sensors. The capacitive midpoint active filter is modeled and simulated to prove that when the voltage of the grid is unbalanced and distorted, the method based on $p-q-r$ do not require a voltage sensor to accurately carry out harmonic detection and fully compensate for the current harmonic components.

Keywords: Filter · Capacitor midpoint · Harmonic detection

1 Introduction

The three-phase four-wire (TF) active filter mainly has a four-leg or capacitive midpoint topology [1]. The four-leg structure has a group of bridge arms more than the capacitive midpoint structure, which is designed to compensate for the midline current, and the compensation effect is better [2]. The small number of switching devices used in the capacitor midpoint has attracted much attention in the small and medium capacity system [3–5], and the medium-line compensation and control strategy for the structure has been the focus of research [6, 7].

The i_p-i_q method based on instantaneous reactive power theory usually introduces a zero-axis decomposition current perpendicular to $p,\ q$ planes, resulting in only active components in the zero-order component, which conflicts with the usual power understanding [6, 8]. The $p-q-r$ method decomposes the voltage and current space vectors under the $p,\ q,\ r$ space coordinate system, defines the active and reactive power of the zero-order components under the TF system, and the various power definitions coincide with the traditional power definitions, while the three power components are completely independent of each other and can be flexibly compensated without the need for energy storage components [3, 9–11]. The effect of midline compensation is improved and the application of the midpoint structure of the capacitor is promoted.

D. Jiang and H. Song (Eds.): SIMUtools 2021, LNICST 424, pp. 359–371, 2022.
https://doi.org/10.1007/978-3-030-97124-3_27

2 Detection Principle of p-q-r

Under the condition of three-phase grid voltage asymmetry, the grid voltage under the a-b-c plane coordinate system is transformed to the three-phase orthogonal α-β-0 spatial coordinate system.

From the Fig. 1

$$e_S = \sqrt{e_\alpha^2 + e_\beta^2 + e_0^2} \tag{1}$$

$$e_{sd} = \sqrt{e_\alpha^2 + e_\beta^2} \tag{2}$$

Voltage synthesis vector e_S is a spatial quantity whose projection on the α-β plane is e_{sd}. Fixed the 0-axis in Fig. 1 (a) to rotate the $\alpha - \beta$ coordinate system counterclockwise angle θ so that the axis α coincides with e_{sd} to obtain axis α_{sd}. The axis β also rotates θ angle to get the q axis, as shown in Fig. 1 (b). Fix the axis q, rotate the $0 - \alpha_{sd}$ coordinate system counterclockwise ϕ so that the axis α_{sd} coincides with the axis e_S to get the axis p and axis r, where the axis q is perpendicular to the $p - q - r$ plane, as shown in Fig. 1(c).

After two coordinate rotations, the spatial $\alpha - \beta - 0$ coordinate system is transformed into a spatial $p - q - r$ coordinate system, transforming matrix A as Eq. (3). After the three-phase current is transformed by matrix A, there is a current component on $p - q - r$ the shaft, such as formula (4). Obviously, in the new spatial coordinate system, the grid voltage space vector is directed to the axis p, and the axis q and axis r do not have a voltage component, so the axis p is an active current axis, the axis q, r is a reactive current axis.

$$A = \frac{1}{e_s}\begin{bmatrix} e_0 & e_\alpha & e_\beta \\ 0 & -e_s e_\beta / e_{sd} & e_s e_\alpha / e_{sd} \\ e_{sd} & -e_0 e_\alpha / e_{sd} & -e_0 e_\beta / e_{sd} \end{bmatrix} \tag{3}$$

$$\begin{bmatrix} e_p \\ e_q \\ e_r \end{bmatrix} = A \begin{bmatrix} e_0 \\ e_\alpha \\ e_\beta \end{bmatrix}, \begin{bmatrix} i_p \\ i_q \\ i_r \end{bmatrix} = A \begin{bmatrix} i_0 \\ i_\alpha \\ i_\beta \end{bmatrix} \tag{4}$$

As can be seen in Fig. 1 (c), the components of the midline current on the axis p and axis r reflect the distribution of the active and reactive components of the midline current. To fully compensate for the midline current, the midline current components on the shaft p and axis r should be offset, i.e.

$$i_{rf} = -i_p tan(\theta_2) = -\frac{e_0}{e_{\alpha\beta}} i_p \tag{5}$$

The current on the p, q shaft is filtered through a low pass, and the resulting DC component corresponds to each phase-based wave component. Therefore, in the three-phase, four-wire harmonic compensation system, the compensation instructions for each axis should be:

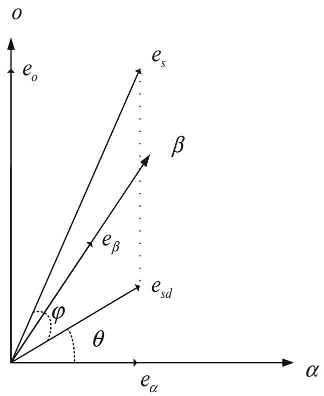

(a) The $\alpha - \beta - 0$ coordinate system

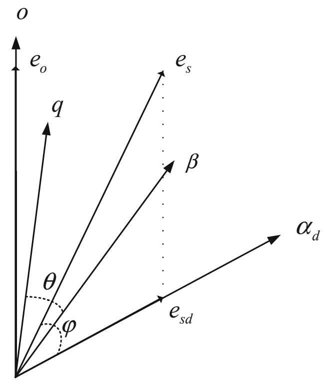

(b) The $\alpha_d - q - 0$ coordinate system

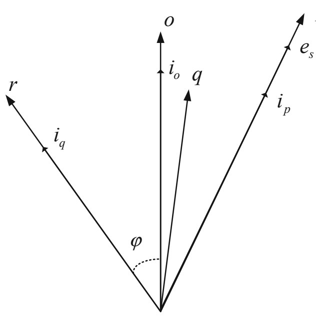

(c) The $p - q - r$ coordinate system

Fig. 1. The formation of a spatial $p - q - r$ coordinate system

The current on the p, q shaft is filtered through a low pass, and the resulting DC component corresponds to each phase-based wave component. Therefore, in the three-phase, four-wire harmonic compensation system, the compensation instructions for each axis should be:

$$\begin{cases} i_{pc} = i_{pac} \\ i_{qc} = i_{qac} \\ i_{rc} = i_r + \frac{e_0}{e_{\alpha\beta}} i_{pdc} \end{cases} \tag{6}$$

In formula (6), i_{pac} is the active current AC component and i_{pdc} is the active current DC component. When the system compensates for reactiveness, according to the advantages of the $p - q - r$ method, the q shaft and shaft r current full compensation can completely compensate for reactive.

Under the condition of grid voltage symmetry, $e_0 = 0$ in the $\alpha - \beta - 0$ coordinate system e_S and e_{sd} coincide in Fig. 1(a). In the spatial $p - q - r$ coordinate system at this time, the axis r and the axis 0 coincide, and to compensate for the midline current, the axis's compensation instruction is $i_{rc} = i_r$.

3 Harmonic Detection Without Voltage Sensor

In the case of system voltage distortion and imbalance, the $p - q - r$ detection method discussed earlier is not able to accurately detect harmonic current.

The following describes the improved $p - q - r$ detection method without the need for voltage sensors and locking rings, which can detect each phase harmonic and midline current in the case of the grid is not ideal and achieve full compensation.

When the voltage is distorted, the symmetrical three-phase grid voltage is:

$$\begin{cases} e_a = \sum\limits_{\infty}^{n=1} \sqrt{2} E_n \, sin(nwt + \theta_n) \\ e_b = \sum\limits_{\infty}^{n=1} \sqrt{2} E_n \, sin[n(wt - \frac{2\pi}{3}) + \theta_n] \\ e_c = \sum\limits_{\infty}^{n=1} \sqrt{2} E_n \, sin[n(wt + \frac{2\pi}{3}) + \theta_n] \end{cases} \tag{7}$$

Where E_n, θ_n are the valid value of each voltage and the initial phase angle is $\theta_1 = 0$. The coordinates are transformed and brought in formula (3) in the event of voltage distortion. Transform the three-phase current i_a, i_b, i_c to get i_α, i_β, i_0, into formula (4), there is:

$$\begin{aligned} i_p &= (e_\alpha i_\alpha + e_\beta i_\beta + e_0 i_0)/e_p \\ i_q &= (e_\alpha i_\beta - e_\beta i_\alpha)/e_{\alpha\beta} \end{aligned} \tag{8}$$

Since e_α, e_β, e_0 all contain 3k harmonics, so that the DC components of i_p and i_q also contain higher secondary harmonics. After the low-pass filter and $C^- A^-$ transformation, i_p and i_q are no longer the fundamental current components of each phase. When the voltage distortion is large, the detection error produced by the $p - q - r$ method is large.

The core of the $p - q - r$ detection method is that E_p in the transformation matrix should represent the positive sequence component of the grid voltage when the vector coordinate transformation is performed. Considering that the point can replace the actual result of power grid voltage detection with a three-phase frequency sine unit vector under the environment of grid voltage distortion, the distortion asymmetric current expression is

$$\begin{bmatrix} i_0 \\ i_\alpha \\ i_\beta \end{bmatrix} = \begin{bmatrix} \sum_{\infty}^{n=1} I_{an}\, sin(nwt + \theta_{an}) \\ \sum_{\infty}^{n=1} I_{bn}\, sin(nwt + \theta_{bn}) \\ \sum_{\infty}^{n=1} I_{cn}\, sin(nwt + \theta_{cn}) \end{bmatrix} \tag{9}$$

In the formula, I_{an} denotes the effective value of a-phase *n-th* harmonic current, θ_{an} denotes the initial phase angle of a-phase *n-th* harmonic current. The improved *A* transform can be obtained (Fig. 2):

$$\begin{aligned} i_p &= \sqrt{3/2} \sum_{\infty}^{n=1} I_{1n}\, cos[(nw - w_1)t + \theta_{1n} - \phi \Big] - \sqrt{3/2} \sum_{\infty}^{n=1} I_{2n}\, cos[(nw + w_1)t + \theta_{2n} + \phi \Big] \\ i_q &= \sqrt{3/2} \sum_{\infty}^{n=1} I_{1n}\, cos[(nw - w_1)t + \theta_{1n} - \phi \Big] + \sqrt{3/2} \sum_{\infty}^{n=1} I_{2n}\, cos[(nw + w_1)t + \theta_{2n} + \phi \Big] \end{aligned} \tag{10}$$

In the case of a small system voltage frequency offset, given that the unit voltage is distributed according to the three-phase frequency sine, then only the base wave component will be included in the DC component of i_p i_q,

$$\begin{bmatrix} i_0 \\ i'_\alpha \\ i'_\beta \end{bmatrix} = C^{-1}A^{-1} \begin{bmatrix} i_{pdc} \\ i_{qdc} \\ i_r \end{bmatrix} = \begin{bmatrix} I_{11}\, sin(wt + \theta_{11}) \\ I_{11}\, sin(wt - 2\pi/3 + \theta_{11}) \\ I_{11}\, sin(wt + 2\pi/3 + \theta_{11}) \end{bmatrix} a \tag{11}$$

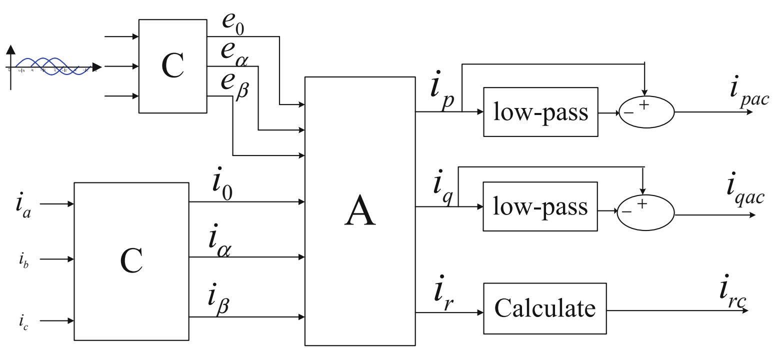

Fig. 2. The improved p-q-r method of detection

4 Simulation Analysis

The $i_p - i_q - i_0$ method is the classical $i_p - i_q$ method in the TF system expansion, The difference between it and the $p-q-r$ method is more reasonably divided from the active and reactive components in the midline current. Both have their own improved models to cope with voltage distortion and asymmetry when the grid voltage is not idealized. Here is the $p - q - r$ method and its improved type as the main research object. The simulation model is established by MATLAB. Figure 3 shows $i_p - i_q - i_0$ method and the simulation model of $p - q - r$ method is shown in Fig. 4.

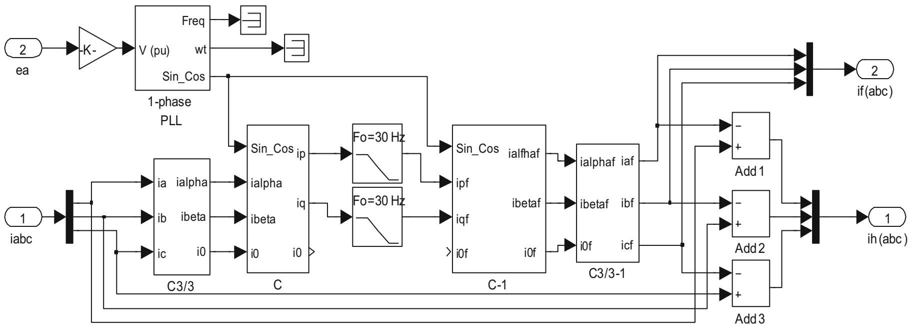

Fig. 3. $i_p - i_q - i_0$ simulation model

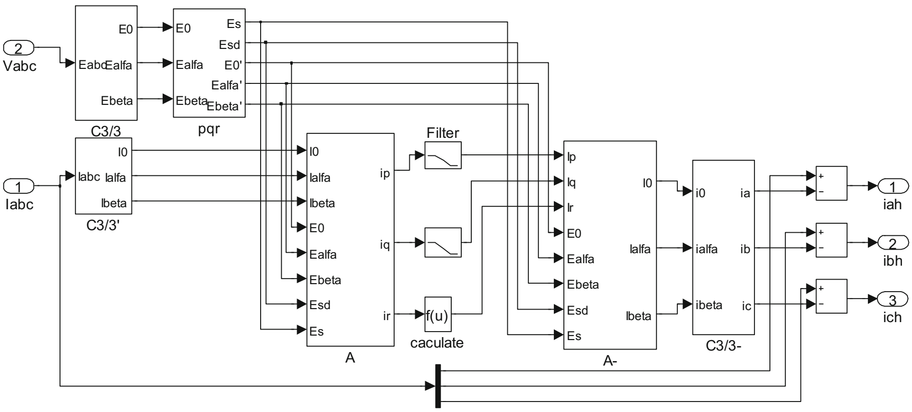

Fig. 4. $p - q - r$ simulation model

4.1 Detection and Analysis of the Ideal Voltage of the Power Grid

The nonlinear load in the simulation is a three-phase non-controlled rectifier bridge, the DC side is connected with two 4 Ω resistors, the middle line is drawn from the midpoint

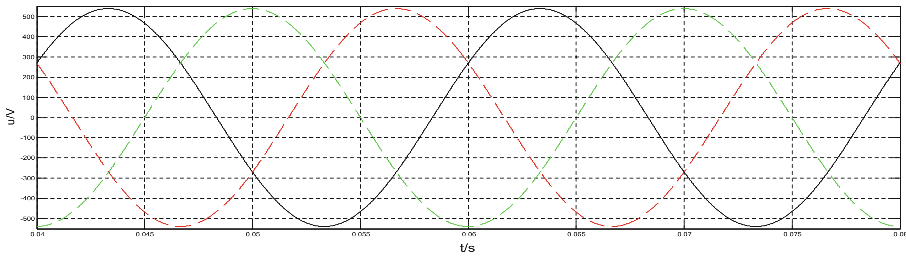

(a) The supply voltage

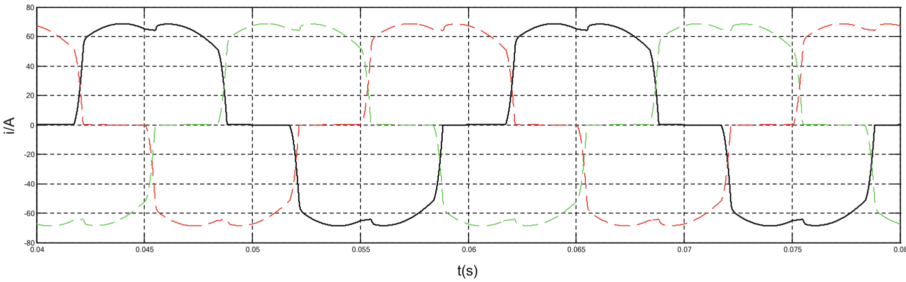

(b) Load current

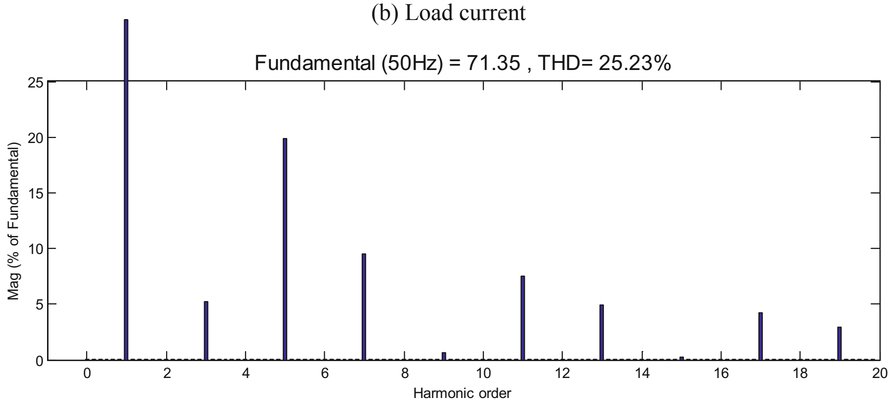

(c) Load current harmonic analysis

Fig. 5. Voltage and load current without distortion of the supply voltage

of the DC side, and the inductance of the AC side of the DC bridge is connected by 0.2 mH.

When the grid voltage is free of distortion, the voltage and current of the load are shown in Fig. 5, which shows that the load current is severely distorted and unbalanced, containing a large number of 6k $\pm$ 1 harmonic.

$i_p - i_q - i_0$ **Detection method**.

$p - q - r$ **Detection method**.

The positive sequence current of the load fundamental detected by $i_p - i_q - i_0$ method and the harmonic current to be compensated are shown in Fig. 6. The positive sequence current of the load fundamental detected by $p - q - r$ and the harmonic current to be compensated are shown in Fig. 7.

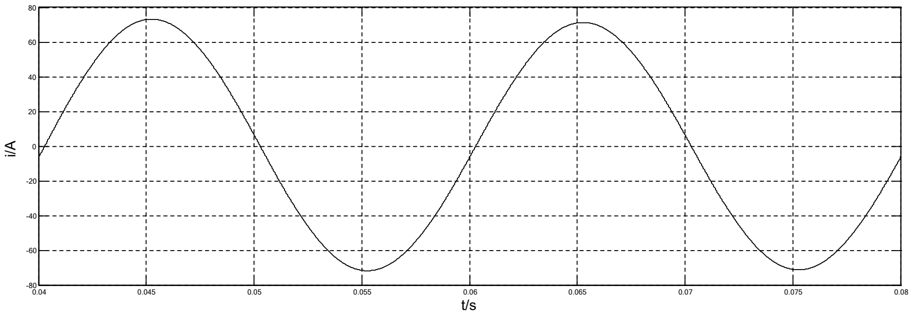

(a) Fundamental positive sequence current of Phase A

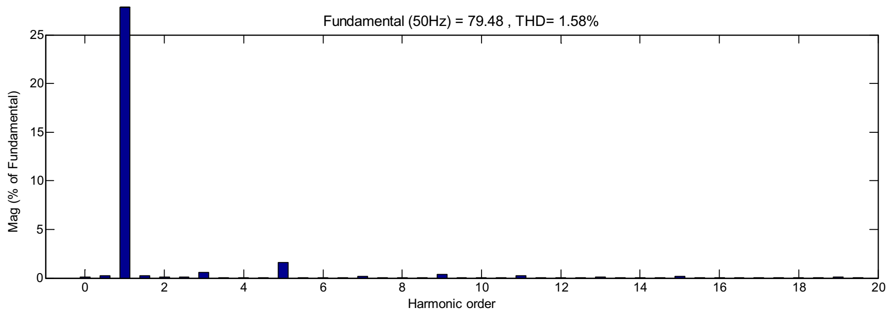

(b) Spectrum of phase A waveform

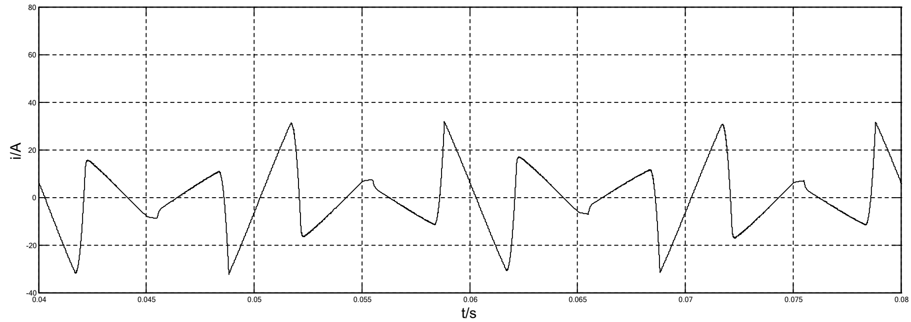

(c) Harmonic current of phase A

Fig. 6. Results of the $i_p - i_q - i_0$ detection method when the supply voltage is free of distortion

The positive current of the load base wave detected by the $i_p - i_q - i_0$ method and the harmonic current to be compensated are shown in Fig. 6. The positive sequential current of the load base wave detected by $p - q - r$ and the harmonic current to be compensated are shown in Fig. 7. The spectrum analysis of the positive current of the base wave captured by the two detection algorithms shows that the distortion rate of the positive sequential current of the a-phase-based wave detected by the $i_p - i_q - i_0$ method is 1.58%, and the distortion rate of the positive-order current of the a-phase-based wave detected by the $p - q - r$ method is 1.50%, which shows that under the ideal condition of the

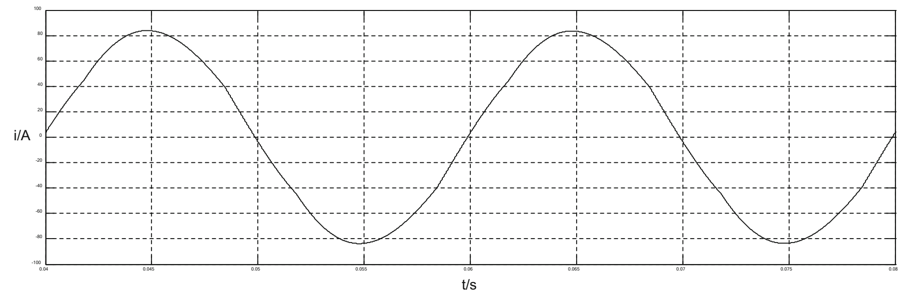

(a) Fundamental positive sequence current of Phase A

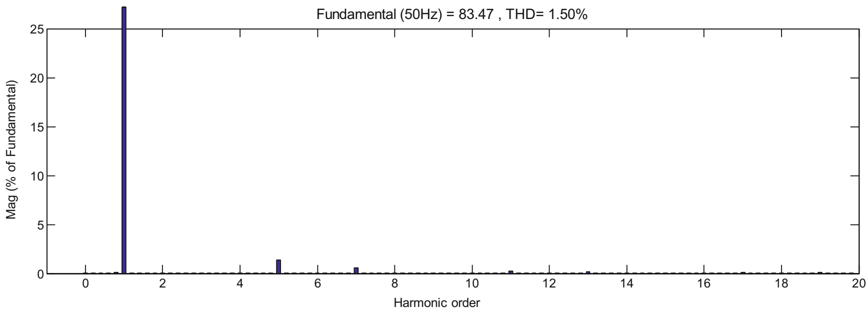

(b) Spectrum of phase A waveform

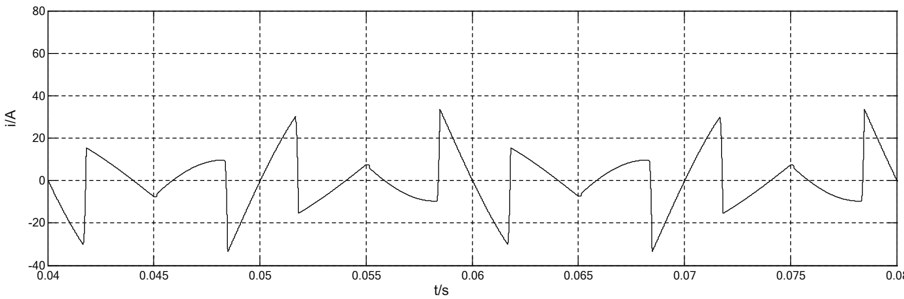

(c) Harmonic current of phase A

Fig. 7. Results of the $p-q-r$ detection method when the supply voltage is free of distortion.

power grid voltage, both the $i_p - i_q - i_0$ method and the $p-q-r$ method can accurately detect the positive current of the base wave, and the effect is not much different.

4.2 Detection and Analysis in the Case of Grid Voltage Imbalance

The input AC voltage fundamental wave effective value $E_{a1} = E_{c1} = 220$ V, $E_{b1} = 150$ V, and the voltage third harmonic effective value $E_{x3} = 30$ V. The load is still a three-phase uncontrolled rectifier bridge, and the middle line is drawn from the DC side. Figure 8 shows the grid voltage and load current waveforms.

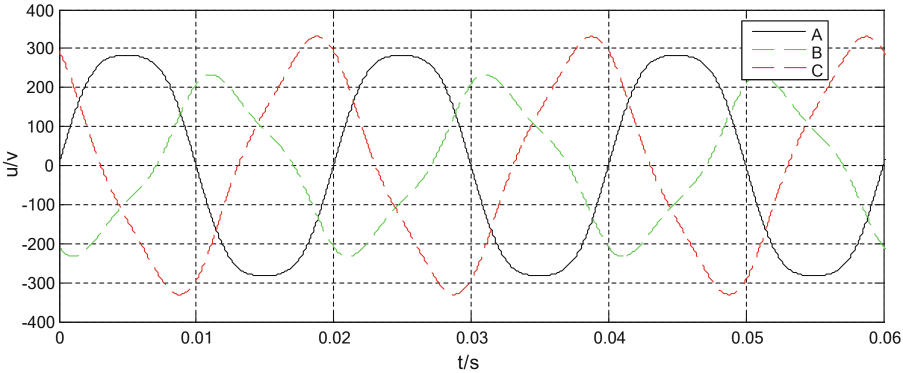

(a) Distortion voltage

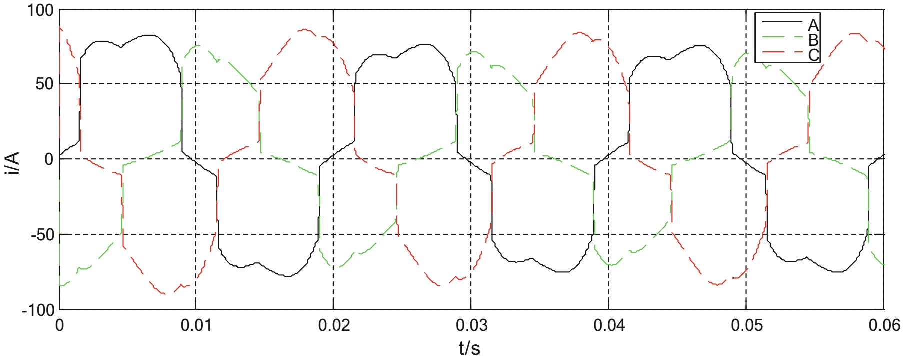

(b) Load current

Fig. 8. Distortion voltage and load current waveforms when grid voltage is unbalanced.

In the case of grid voltage imbalance, the improved $p-q-r$ method uses unit sine signal instead of the real-time grid voltage detected by the voltage sensor, and the resulting a-phase and b-phase-based wave spectrum is shown in Fig. 9(b) and (c), which can detect harmonic currents in real-time. Figure 10 is the application of $p-q-r$ harmonic detection method to compensate for the front and rear waveforms of the midline current, indicating that the method is good for the midline current compensation effect.

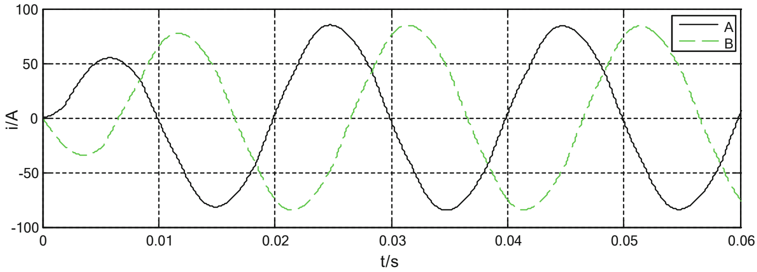

(a) Fundamental positive sequence current of Phase A

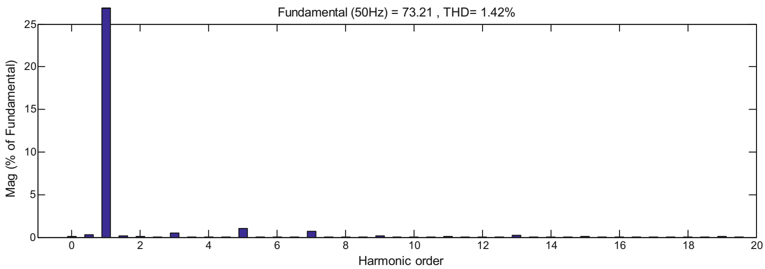

(b) Spectrum of phase A waveform

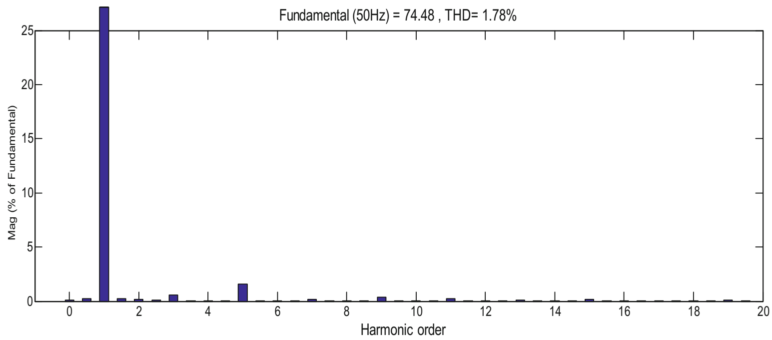

(c) Spectrum of phase B waveform

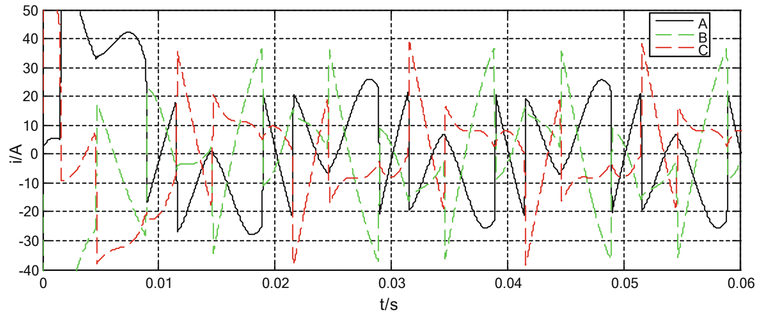

(d) Harmonic instruction current

Fig. 9. The results of the $p - q - r$ detection method when the voltage of the power grid is unbalanced.

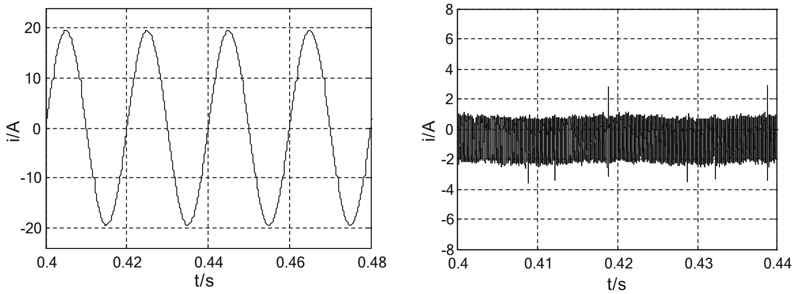

Fig. 10. The midline current compensates for the front and rear waveforms

5 Conclusion

This paper mainly introduces the basic principle of $p-q-r$ harmonic detection method under the TF system, and puts forward the $p-q-r$ harmonic detection method of voltage-free sensor. Simulation proves that the improved $p-q-r$ detection method does not require a voltage sensor, and the positive sequence components and harmonic components of the current-based wave of the grid can still be correctly detected in the case of uneven grid voltage. The capacitor midpoint active power filter uses the harmonic detection method to compensate the midline current well, which greatly simplifies the engineering difficulty and cost, and promotes the popularization and application of capacitive structure active power filter.

Acknowledgement. The authors acknowledge the Jiangsu University Natural Science Research Project (18KJB470024) and Funding Project for Professional Leaders of Higher Vocational Colleges in Jiangsu Province (2020GRGDYX070). This work was supported by the practice and innovation project of Jiangsu Vocational Institute of Architectural Technology in 2019 (JYSCZ19-10).

References

1. Beres, R.N., Wang, X., Liserre, M., Blaabjerg, F., Bak, C.L.: A review of passive power filters for three-phase grid-connected voltage-source converters. IEEE J. Emerg. Sel. Top. Power Electron. **4**(1), 54–69 (2016). https://doi.org/10.1109/JESTPE.2015.2507203
2. Wang, X.Q., Zhao, J.W., Wang, Q.J., Li, G.L., Zhang, M.S.: Improved three-phase four wire harmonic detection method. Dianji yu Kongzhi Xuebao/Electr. Mach. Control **24**(9), 84–94 (2020). https://doi.org/10.15938/j.emc.2020.09.010
3. Kang, Y.K., Jung, H.G., Lee, K.B.: Control method in a wind turbine driven by 3-parallel back-to-back converters using PQR power transformation. In: 2010 International Power Electronics Conference - ECCE Asia -, IPEC 2010, pp. 2562–2568 (2010). https://doi.org/10.1109/IPEC.2010.5542356
4. Hasim, A.S.B.A., Dardin, S.M.F.S., Ibrahim, Z.B., Azid, A.B.A., Ishak, A.M.B.: Comparative study; different types of PWM control scheme in three-phase four-wire shunt active power filter (APF) topology (2019). https://doi.org/10.1109/ICECOS.2018.8605234

5. Ben Braiek, M.L., Fnaiech, F., Al-Haddad, K., Yacoubi, L.: Comparison of direct current control techniques for a three-phase shunt active power filter. In: IEEE International Symposium on Industrial Electronics, vol. 4 (2002). https://doi.org/10.1109/isie.2002.1025963
6. Li, D.: Study on control strategy and application of a new harmonic detection method in three-phase four-wire APF. Concurr. Comput. **31**(10), e4853 (2019). https://doi.org/10.1002/cpe.4853
7. Bao, L., Xia, J., Dong, Z., Deng, Y., Lu, Y., Yang, Y.: An improved three-phase four-wire harmonic detection algorithm based on multi-synchronous rotating frame transformation. In: IECON Proceedings (Industrial Electronics Conference), vol. 2019, pp. 2115–2120 (2019). https://doi.org/10.1109/IECON.2019.8927561
8. Wang, G., Chang, W., Bak, C.L., Zhou, M., Hao, Z.: Control strategy for combined co-phase power supply system based on theory of control without harmonic detection and selective harmonic compensation. Dianli Zidonghua Shebei/Electr. Power Autom. Equip. **37**(12), 130–137 (2017). https://doi.org/10.16081/j.issn.1006-6047.2017.12.018
9. Yuniantoro, I., Gunawan, R., Setiabudy, R.: The PQR-coordinate in the mapping matrices model of Kim-Akagi on power transformation based on Euler angle rotation method. In: 2013 International Conference on Quality in Research, QiR 2013 - In Conjunction with ICCS 2013: The 2nd International Conference on Civic Space, pp. 121–126 (2013). https://doi.org/10.1109/QiR.2013.6632549
10. Lee, S.J., Kim, H., Sul, S.K., Blaabjerg, F.: A novel control algorithm for static series compensators by use of PQR instantaneous power theory. IEEE Trans. Power Electron. **19**(3), 814–827 (2004). https://doi.org/10.1109/TPEL.2004.826499
11. Kim, H., Lee, S.J., Sul, S.K.: Reference wave generation in dynamic voltage restorers by use of PQR power theory. In: Conference Proceedings - IEEE Applied Power Electronics Conference and Exposition - APEC, vol. 3, pp. 1452–1457 (2004). https://doi.org/10.1109/apec.2004.1296055